Smooth muscle cell rigidity and extracellular matrix organization influence endothelial cell spreading and adhesion formation in coculture

Charles S. Wallace, Sophie A. Strike, and George A. Truskey

Department of Biomedical Engineering, Duke University, Durham, North Carolina

Submitted 27 May 2007; accepted in final form 17 July 2007

Wallace CS, Strike SA, Truskey GA. Smooth muscle cell rigidity and extracellular matrix organization influence endothelial cell spreading and adhesion formation in coculture. *Am J Physiol Heart Circ Physiol* 293: H1978–H1986, 2007; doi:10.1152/ajpheart.00618.2007.—Efforts to develop functional tissue-engineered blood vessels have focused on improving the strength and mechanical properties of the vessel wall, while the functional status of the endothelium within these vessels has received less attention. Endothelial cell (EC) function is influenced by interactions between its basal surface and the underlying extracellular matrix. In this study, we utilized a coculture model of a tissue-engineered blood vessel to evaluate EC attachment, spreading, and adhesion formation to the extracellular matrix on the surface of quiescent smooth muscle cells (SMCs). ECs attached to and spread on SMCs primarily through the $\alpha_5\beta_1$-integrin complex, whereas ECs used either $\alpha_5\beta_1$- or $\alpha_v\beta_3$-integrin to spread on fibronectin (FN) adsorbed to plastic. ECs in coculture lacked focal adhesions, but EC $\alpha_5\beta_1$-integrin bound to fibrillar FN on the SMC surface, promoting rapid fibrillar adhesion formation. As assessed by both Western blot analysis and quantitative real-time RT-PCR, coculture suppressed the expression of focal adhesion proteins and mRNA, whereas tensin protein and mRNA expression were elevated. When attached to polyacrylamide gels with similar elastic moduli as SMCs, focal adhesion formation and the rate of cell spreading increased relative to ECs in coculture. Thus, the elastic properties are only one factor contributing to EC spreading and focal adhesion formation in coculture. The results suggest that the softness of the SMCs and the fibrillar organization of FN inhibit focal adhesions and reduce cell spreading while promoting fibrillar adhesion formation. These changes in the type of adhesions may alter EC signaling pathways in tissue-engineered blood vessels.

focal adhesions; fibrillar adhesions; tissue engineering; integrin; elastic modulus

DURING THE PAST DECADE, there have been great strides toward creating a clinically viable tissue-engineered blood vessel (TEBV) (12). While most studies have focused on improving the strength and mechanical properties of the vessel wall, the functional status of the endothelium within these TEBVs has received less attention, despite having a critical role in vasodilation, platelet coagulation and clot formation, immune response, and water and solute permeability (3).

Endothelial cell (EC) function is influenced by interactions between integrins on the basal surface and the underlying extracellular matrix (ECM) (9, 21). The integrins involved with attachment and the proteins that interact with the cytoplasmic domains of these integrins determine the type of adhesion that is formed. These adhesions include nascent focal complexes that form during cell spreading, classical focal adhesions, and elongated and elliptical fibrillar adhesions that arise when

fibrillar fibronectin (FN) forms (for a review, see Ref. 32). Late focal complexes and focal adhesions consist of many of the same proteins, such as $\alpha_v\beta_3$-integrin, vinculin, paxillin, and focal adhesion kinase (FAK); in contrast, fibrillar adhesions lack the aforementioned proteins and are rich in $\alpha_5\beta_1$-integrin and tensin. Tensin can also be found in focal adhesions. Focal adhesions are primarily located at the cell periphery with very low colocalization with FN fibrils, whereas fibrillar adhesions form along FN fibrils and are located in the central portion of the cell (14).

Zamir et al. (33) and others (for a review, see Ref. 6) showed that when cells initially attach to the substrate, integrins cluster and the properties of the substrate determine the type of adhesions that are formed. If the underlying FN matrix is deformable, then fibrillar adhesions will form (14). If the substrate is rigid and contains a nondeformable matrix, then the immobilized adhesion complexes produce high tension that induces the formation of focal adhesions (14). The types of adhesions the ECs create and the integrins involved can affect EC function (9, 21).

In vivo and with TEBVs, ECs adhere to the ECM and underlying SMCs that are much softer than the substrates used for two-dimensional culture in vitro. We (28) developed and characterized a direct coculture system as a mimic of TEBVs. In coculture, SMCs organize FN into fibrils prior to the attachment of ECs. Thus, these substrate conditions in coculture and TEBVs may affect the adhesion of ECs. In this study, we tested the hypothesis that the substrate conditions in coculture reduce EC focal adhesion formation and promote the formation of fibrillar adhesions. To quantitatively assess this hypothesis, we compared EC adhesion on SMCs with EC adhesion on tissue culture plastic or polyacrylamide surfaces of different elastic moduli.

MATERIALS AND METHODS

Media composition and coculture formation. All media were supplemented with 1× antibiotic-antimycotic (GIBCO-BRL, Carlsbad, CA). Human aortic SMCs (Cambrex, Walkersville, MD) were expanded with SMC growth media containing smooth muscle basal media (SmBM; Cambrex) supplemented with SmGM-2 singleQuots (Cambrex). To switch SMCs from a proliferative state to a quiescent state, SMCs were maintained in serum-free quiescent media composed of DMEM-F-12 (GIBCO-BRL) supplemented with 1× insulin-transferrin-selenium (GIBCO-BRL). Human aortic ECs (Cambrex) were expanded in endothelial basal media-2 (EBM-2; Cambrex) supplemented with EGM-2 SingleQuots (Cambrex). Cocultures were maintained in a coculture medium composed of medium 199 (GIBCO-BRL) supplemented with 5.5% human serum (Sigma, St.

Louis, MO) and 1× insulin-transferrin-selenium (GIBCO-BRL). All cells were trypsinized with 0.025% trypsin-EDTA (Clonetics) for 5 min at 37°C except when ECs were separated from SMCs in coculture.

To prepare cocultures, SMCs were plated at 75,000 cells/cm^2 on tissue culture plastic dishes (Corning, Corning, NY) or polystyrene slideflasks (NUNC, Rochester, NY) that were incubated with 3.3 μg/ml human plasma FN (Sigma) for over 1 h. SMCs (*passages 7–11*) were grown to confluence in SMC growth media, forming one to three layers. Two days after SMCs had been seeded, media were changed from SMC growth media to SMC quiescent media. Two days after the addition of the quiescent media, human aortic ECs (*passages 7–10*) were seeded at a confluent density (75,000–100,000 cells/cm^2) directly on top of the quiescent SMCs in EC growth media except where noted. After ~24 h, media were changed to coculture media. All cell cultures were maintained in a tissue culture incubator at 37°C and 5% CO$_2$, and the medium was exchanged every other day.

Imaging ECs and SMCs in coculture. To visualize cells, ECs were stained with DiI-Ac-LDL (5 μg/ml, 4 h, 37°C; Biomedical Technologies, Stoughton, MA) while in coculture or with CellTracker orange (2 μM, 10 min, 37°C; Invitrogen, Carlsbad, CA) before being plated.

Fluorescent images were obtained with a confocal laser scanning microscope (LSM 510, Carl Zeiss, Thornwood, NY) or an inverted fluorescent microscope (Zeiss Axiovert S-100, Carl Zeiss) connected to a digital camera (Carl Zeiss). The camera was connected via a frame grabber card (Pr-LG3-01 PCI, Scion, Frederick, MD) to a Macintosh G3 computer (Apple Computer, Cupertino, CA).

Blocking EC attachment. The EC integrins involved with the initial attachment of ECs to SMCs were determined utilizing monoclonal integrin blocking antibodies. Approximately 200,000 ECs, labeled with CellTracker orange, were suspended in 250 μl of Dulbecco's PBS solution (DPBS; GIBCO-BRL) and rotated in a 1.5-ml tube in the tissue culture incubator for 30 min with no antibodies, 5 μl of mouse anti-human $\alpha_5\beta_1$-integrin (Chemicon, Temecula,CA), mouse anti-human $\alpha_v\beta_3$-integrin (Chemicon), or a combination of the two antibodies. Next, the cell suspension was combined with 1.75 ml of DPBS and added to either quiescent SMCs or 12-well tissue culture plates that were first incubated with 3.3 μg/ml FN for 1 h, rinsed, and incubated with 1% BSA for 1 h to block nonspecific binding. After a 10-min incubation at 37°C, nonadherent ECs were removed with three DPBS rinses, and adherent cells were fixed with 3.7% paraformaldehyde for 15 min at 37°C. Ten random fluorescent images were captured per sample, and numbers of attached ECs were measured with a custom cell counting Matlab (version 7.0, The MathWorks, Natick, MA) program.

EC spreading. To determine the spreading rate of ECs plated on SMCs or polyacrylamide gels, ECs were stained with CellTracker orange and plated at 20,000 cells/cm^2 in the fully supplemented EBM-2 media. After 30, 75, 120, and 165 min of attachment, approximately six fluorescent images were captured. Image J (version 1.36, National Institutes of Health) was used to trace and measure the cell area of at least 30 ECs per time point. A linear regression between EC area and attachment time was performed to determine the rate of EC spreading.

To block EC spreading, the following antibodies, at a dilution of 1:100, were added to the media after ECs attached and spread for 5 min: no antibody (control), mouse anti-human $\alpha_5\beta_1$-integrin (Chemicon), mouse anti-human $\alpha_v\beta_3$-integrin (Chemicon), or a combination of the two antibodies. After 1 h of spreading, cultures were fixed with 3.7% paraformaldehyde and imaged. The cell areas of at least 50 ECs were measured per experiment using ImageJ.

Immunofluorescence. Cells were fixed with 3.7% paraformaldehyde for 15 min at 37°C and permeabilized with 0.2% Triton X-100 (Sigma) at room temperature for 5 min. Cells were rinsed with DPBS and then incubated with 10% goat serum (Sigma) for 30 min at 37°C to block nonspecific binding. Primary antibodies [vinculin, 1:100 (Sigma); paxillin, 1:400 (Invitrogen); PY20, 1:100; FN, 1:200; and

tensin, 1:25 (BD Biosciences-Pharmingen, San Diego, CA)] were incubated with the cells for 1 h at 37°C in 10% goat serum. Cells were rinsed multiple times and then incubated at 37°C for 45 min in 10% goat serum with Alexa fluor 488 or 546 goat anti-mouse secondary antibody (1:500, Invitrogen). The focal adhesion area was measured by capturing at least 6 images/sample of the vinculin immunofluorescence and using ImageJ to trace and measure the area of at least 30 random focal adhesions/sample.

Green fluorescent protein-vinculin and -tensin expression. Green fluorescent protein (GFP)-vinculin and GFP-tensin plasmids (provided by S. Lin, D. Lin, and K. Yamada) were selected by ampicillin resistance and amplified in *Escherichia coli* (DH5α, Invitrogen). ECs were transfected with the GFP-plasmid using a liposomal method (Lipofectin Transfection Reagent, Invitrogen) according to the manufacturer's protocols. Briefly, ECs were grown to 50–70% confluence in six-well plates before transfection; 1 μg/ml of plasmid and 7 μl/ml of Lipofectin were mixed and incubated with Opti-MEM I (Invitrogen) for 20 min to form plasmid-Lipofectin complexes. ECs were then incubated for 2.5 h with Opti-MEM I containing the plasmid-Lipofectin complexes. The medium was exchanged with EC growth media, and cells were allowed to recover overnight.

Separation of ECs from SMCs for total RNA and protein isolation. Cocultures were washed with DPBS without Ca^{2+} and Mg^{2+} to remove media proteins. A 5-min wash was then performed with ice-cold DPBS without Ca^{2+} and Mg^{2+}. This caused the ECs to contract slightly due to the drastic temperature change, thus allowing more of the trypsin to access EC integrins. Trypsin-EDTA (0.25%) at 37°C was then added to the cells for 5 min. Trypsin was neutralized with Trypsin Neutralizing Solution (Clonetics), and the cell suspension was pipetted multiple times to break any remaining bonds between cells. Cells were pelleted and resuspended with 1 ml of 0.1% BSA in DPBS. ECs and SMCs were then separated using magnetic beads.

A volume of 25 μl of CD31 EC Dynabeads (Invitrogen) was mixed with the cell sample for 20 min at room temperature. The bead-cell solution was placed in the Dynal MPC Magnet (Invitrogen), where the EC-bead complex was pulled to the side of the magnet and the supernatant (SMCs in suspension) was removed. EC-bead complexes were resuspended in 0.1% BSA in DPBS. The solution was placed in the magnet, and the supernatant was discarded. ECs were then washed three more times to increase EC purity. The magnetic bead separation technique yielded an EC purity of 98.7 ± 0.4, which was determined by identification of positive Ac-LDL-DiI staining of separated ECs (*n* = 3). Purified ECs were then lysed with lysis buffer for either RNA or protein isolation.

Total EC RNA was isolated from the EC-bead complex using a commercially available RNA isolation kit (High-Pure Total RNA Isolation Kit, Roche Applied Science, Indianapolis, IN). Total EC protein was isolated with Cell Lytic-M (Sigma) supplemented with Protease Inhibitor Cocktail (1:10, Sigma). The protein lysis buffer was rotated with the EC-bead complexes for 15 min at 4°C, and the cell debris and beads were pelleted with centrifugation so that the lysate could be isolated.

Quantitative real-time RT-PCR. RNA purity and quantity were measured using a NanoDrop Spectrophotometer (NanoDrop Technologies, Wilmington, DE). Total RNA (50 ng) was reverse transcribed using the cDNA Synthesis Kit (Bio-Rad, Hercules, CA) and a MyCycler (Bio-Rad) thermal cycler. One cycle of 5 min at 25°C, 30 min at 43°C, and 5 min at 85°C was performed. Primers (Integrated DNA Technologies, Coralville, IA), RNAse free water, and IQ SYBR Green Supermix (Bio-Rad) were combined with the cDNA samples and placed in a MyIQ Single Color Real-Time PCR Detection System (Bio-Rad). A two-step cycle configuration was performed with an initial denaturation for 3 min at 95°C and 50 cycles at 95°C for 15 s and 61°C for 1 min. All samples were performed in triplicate for all genes. The $2^{-\Delta\Delta C_T}$ method was used to determine relative gene expression (17), where C$_T$ is threshold cycle. Primers were selected based on the gene sequence (Pub-Med) of interest and using

Primer3 shared software (23). The primers used were as follows: *1*) β2-microglobulin, 5′-GGCTATCCAGCGTACTCCAAAG-3′ and 5′-CAACTTCAATGTCGGATGGATG-3′; *2*) α-actinin, 5′-GGCAA-GATGAGAGTGCACAA-3' and 5′-AGATGTCCTGGATGGCAAAG-3′; *3*) paxillin, 5′-TGATAGGATTTGGGGCAGAG-3' and 5′-CCAGT-GGAGTGGTTTGGACT-3′; *4*) tensin, 5′-GGCTTAGAGCGAGA-GAAGCA-3' and 5′-CCCGTCCAGAGAAGAGAGTG-3′; *5*) vinculin: 5′-CTTTGCTGCTACAGGGGAAG-3' and 5′-GGATATGGGACGG-GAAGTTT-3′; *6*) FAK, 5′-TTATTGGCCACTGTGGATGA-3′ and 5′-TACTCTTGCTGGAGGCTGGT-3′; and *7*) RhoA, 5′-AAGGAC-CAGTTCCCAGAGGT-3′ and 5′-TTCTGGGGTCCACTTTTCTG-3′.

Western blot analysis. The BCA protein assay (Sigma) was used to determine the protein concentration in the lysate. Protein lysate (20 μg) was boiled with Lamaelli sample buffer (1:1, Bio-Rad) for 5 min. The resulting solution was then added to a 7.5% Tris·HCl Ready-Made gel (Bio-Rad), and electrophoresis was completed at 150 V for ~35 min. A wet transfer (Towbin buffer) was completed at 100 V and 90 mA for 1 h to transfer vinculin and paxillin from the gel to a polyvinylidene difluoride (PVDF) membrane. Tensin was transferred in Towbin buffer with 20% methanol and 0.05% SDS for 3 h at 500 mA. The membrane was blocked for 1 h with 5% milk. The primary antibody reactive to the protein of choice was incubated with the PVDF membrane overnight at 4°C (vinculin, 1:1,000; paxillin, 1:1,000; and tensin, 1:150) in 1% milk. After multiple washes with Tris-buffered saline (TBS)-Tween solution, the membrane was incubated with a secondary antibody (anti-mouse IgG-horseradish peroxidase, Santa Cruz Biotechnology) in 5% milk at 1:5,000 dilution for 1 h. Enhanced chemiluminescence (Pierce) solution was added to the membrane for 5 min, and the membrane was exposed to CL-XPosure Film (Pierce). Bands were then analyzed using the gel analyzer macro in ImageJ.

Atomic force microscopy. Samples were probed with an Asylum 1-D Atomic Force Microscope (AFM; Asylum Research, Santa Barbara, CA) in contact mode. A long narrow hydrophilic borosilicate cantilever with a spherical tip (radius = 2.5 μm; Bioforce Nanoscience, Ames, IA) and a nominal spring constant of 60 pN/nm was used to contact the sample. The actual spring constant was determined by a thermal fluctuations method. Samples were probed approximately seven times at random locations. The indentation (δ) was obtained by subtracting the deflection from the movement of the piezoelectric ceramic (*z*) as follows: δ = z − z₀, where z₀ is the initial deflection. Force-deflection curves for the polyacrylamide gels and SMCs were obtained using IGOR Pro 5.04B (Wavemetrics, Portland, OR). Since cells are viscoelastic and the mechanical properties vary spatially, the apparent modulus *E** was calculated by fitting the force-indentation curves to the following equation:

$$F = \frac{4E^*}{3(1 - \nu^2)} R^{1/2} \delta^{3/2} \qquad (1)$$

where F is the force, E^* is Young's modulus, ν is Poisson's ratio [a value of 0.5 is commonly used for cells (25) and polyacrylamide gels (7)], and *R* is the radius of the sphere on the tip. To minimize viscous contributions, we indented at 2 μm/s. All plots of force versus $\delta^{3/2}$ had correlation coefficients above 0.98.

Polyacrylamide gel preparation and FN cross-linking. Polyacrylamide gels were prepared on glass slides as described by Pelham and Wang (22). Briefly, glass slides were treated with aminopropyltrimethoxysilane and 0.5% glutaraldehyde to create a surface that would firmly adhere to the gel. Mixtures consisting of 5% acrylamide and 0.025–0.1% bis-acrylamide were prepared by mixing 40% acrylamide, 1 M HEPES, 2% bis-acrylamide, and distilled water. Acrylamide solutions were degassed for 20 min to remove oxygen that could inhibit the polymerization of acrylamide. Next, 10% ammonium persulfate and *N,N,N′,N′*-tetramethylethylenediamine were added to the acrylamide solution to catalyze the cross-linking of the polymer. A volume of 15 μl of the acrylamide solution was pipetted onto the aminosilanized glass slides. A 22-mm-diameter circular glass coverslip was immediately placed over the solu-

tion, and gels were allowed to polymerize for 30 min before being rinsed with 50 mM HEPES and removal of the coverslip. Gels were stored in 50 mM HEPES at 4°C and used within 2 wk.

To immobilize FN, a cross-linker, *N*-sulfosuccinimidyl-6-(4′-azido-2′-nitrophenylamino)-hexanoate (sulfo-SANPAH; Pierce), was added to the surface of the gels at a concentration of 0.5 mg/ml. Sulfo-SANPAH was activated by placing the gels ~3 in. from four 7.5-W tubes of 302-nm UV light for 8 min. Gels were rinsed, and the UV cross-linking was repeated. Next, gels were incubated with 10 μg/ml FN overnight at 4°C and rinsed with DPBS. To increase the amount of FN matrix, some gels underwent three additional incubations with 10 μg/ml FN for 1 h each at 37°C. FN-coated gels were stored for <1 wk at 4°C before being used.

Statistical analysis. ANOVA was performed when making multiple comparisons and a Tukey-Kramer analysis was used as a post hoc test. Student's *t*-test was performed when only two groups of data were compared. A value of $P < 0.05$ was considered statistically significant. Data are expressed as means ± SE.

RESULTS

α₅β₁-Integrin controls EC attachment and spreading on SMCs. The numbers of ECs that attached to SMCs or FN-coated plastic were significantly reduced by blocking the α₅β₁-integrin complex ($n = 3$–5; Fig. 1*A*). In contrast, the addition of a blocking antibody to αᵥβ₃-integrin alone did not affect EC
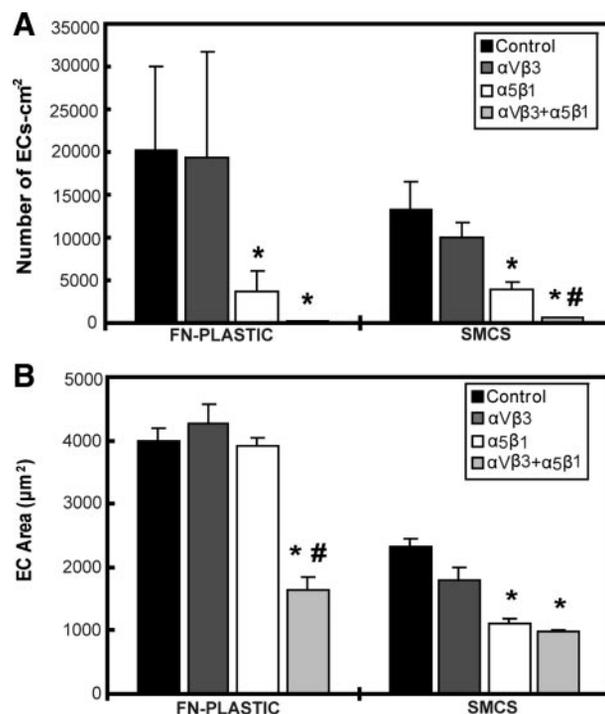

Fig. 1. Integrin blocking antibodies were used to determine the effect of α₅β₁- and αᵥβ₃-integrin in endothelial cell (EC) attachment and spreading on fibronectin (FN)-coated plastic and smooth muscle cells (SMCs) ($n = 3$–5). ECs attached to and spread along SMCs primarily through their FN receptor (α₅β₁-integrin). α₅β₁-Integrin blocking antibodies significantly reduced the numbers of ECs that initially attached to FN-coated plastic or SMCs, and the combination of α₅β₁- and αᵥβ₃-integrin blocking antibodies fully inhibited EC adherence to SMCs and FN-coated plastic (*A*). EC spreading on FN-coated plastic was reduced only when both α₅β₁- and αᵥβ₃-integrin complexes were simultaneously blocked, whereas EC spreading on SMCs was reduced when α₅β₁-integrin was blocked. Blocking both α₅β₁- and αᵥβ₃-integrin complexes in coculture did not further reduce EC spreading compared with only blocking α₅β₁-integrin alone (*B*). *$P < 0.05$ compared with control; #$P < 0.05$ compared with α₅β₁-integrin treatment.

attachment. EC attachment to SMCs or FN-coated plastic was fully inhibited by simultaneously blocking $\alpha_5\beta_1$- and $\alpha_v\beta_3$-integrin on both substrates. Thus, ECs attached to SMCs with the same integrins involved in the attachment to FN-coated plastic, suggesting that FN on the surface of SMCs (28) is the major ECM protein influencing EC attachment in coculture.

EC spreading on FN-coated plastic was significantly reduced only by simultaneously blocking $\alpha_5\beta_1$- and $\alpha_v\beta_3$-integrin, whereas blocking only $\alpha_5\beta_1$-integrin significantly reduced EC spreading on SMCs ($n = 5$; Fig. 1B). Simultaneously blocking $\alpha_5\beta_1$- and $\alpha_v\beta_3$-integrin did not further reduce EC spreading on SMCs compared with blocking $\alpha_5\beta_1$-integrin alone. These results suggest that ECs used either $\alpha_5\beta_1$- or $\alpha_v\beta_3$-integrin complexes to spread on FN-coated plastic, but ECs spread on SMCs primarily through the $\alpha_5\beta_1$-integrin complex. Also, after 1 h of spreading, control ECs on SMCs were approximately half the size of control ECs on FN-coated plastic.

ECs form focal complexes on SMCs and on FN-coated plastic. Since EC spreading on SMCs was significantly reduced compared with EC spreading on FN-coated plastic (28), we hypothesized that there were differences in focal complex formation. The formation of focal complexes was determined by the positive staining of phosphotyrosine, paxillin, and vinculin along the cell periphery (Fig. 2). After 1 h of spreading, ECs that adhered to SMCs had similar amounts of phosphotyrosine and paxillin at the cell periphery as ECs in monoculture, but there was a noticeable decrease in vinculin recruitment at the cell periphery of ECs in coculture. Also, after 1 h of spreading, ECs in monoculture formed some focal adhesions, but focal adhesion formation was not found in coculture.

ECs on SMCs form fibrillar adhesions and lack focal adhesions. As cell spreading progresses, focal complexes mature into focal adhesions due to the tension generated along the actin filaments within the cell (for a review, see Ref. 24). Consistent with the literature, subconfluent ECs expressing GFP-vinculin formed focal adhesions 4 h after attachment when adhered to FN-coated plastic (Fig. 3A). In contrast, subconfluent ECs adhered to SMCs did not form focal adhe-

sions. To assess whether focal adhesions formed at later times in coculture, we used immunofluorescence to identify focal adhesions 2 days after attachment (not shown). Again, ECs adhered to FN-coated plastic formed focal adhesions. ECs adhered to SMCs did not form focal adhesions, although SMCs in coculture did form focal adhesions to the underlying plastic substrate. ECs in coculture lacked vinculin and paxillin plaques, but staining revealed that both of these proteins were diffusely present within cells.

Due to the presence of FN fibrils on the surface of SMCs (28) and the role of $\alpha_5\beta_1$-integrin in EC spreading, we hypothesized that ECs in coculture formed fibrillar adhesions. Subconfluent ECs expressing GFP-tensin formed fibrillar adhesions after 4 h of spreading when adhered to SMCs, as indicated by the centrally located elongated tensin plaques (Fig. 3A). In contrast, subconfluent ECs adhered to FN-coated plastic did not form fibrillar adhesions after 4 h of attachment. The small tensin plaques present in the monoculture at the 4-h time point resembled focal adhesions and not fibrillar adhesions due to their small size and location at the cell periphery. After 2 days of attachment, fibrillar adhesion formation was found in coculture, as indicated by the elongated pattern of tensin immunofluorescence, whereas EC fibrillar adhesions were not found in monoculture (not shown). ECs in monoculture did seem to have more tensin plaques after 2 days compared with 4 h of attachment. Consistent with this observation, FN between ECs and SMCs in coculture remained in a fibrillar organization (28), whereas ECs in monoculture had only started to reorganize the FN into fibrils (Fig. 3B). Thus, ECs rapidly formed fibrillar adhesions in coculture due to the presence of fibrillar FN on the surface of SMCs.

To assess whether the lack of focal adhesion formation in coculture led to a reduction in focal adhesion proteins, the amounts of vinculin and paxillin within confluent ECs were quantified by Western blot analysis 2 days after the onset of coculture ($n = 3$; Fig. 4A). Vinculin and paxillin protein expression within ECs in coculture were significantly lower than ECs in monoculture, whereas ECs in coculture expressed
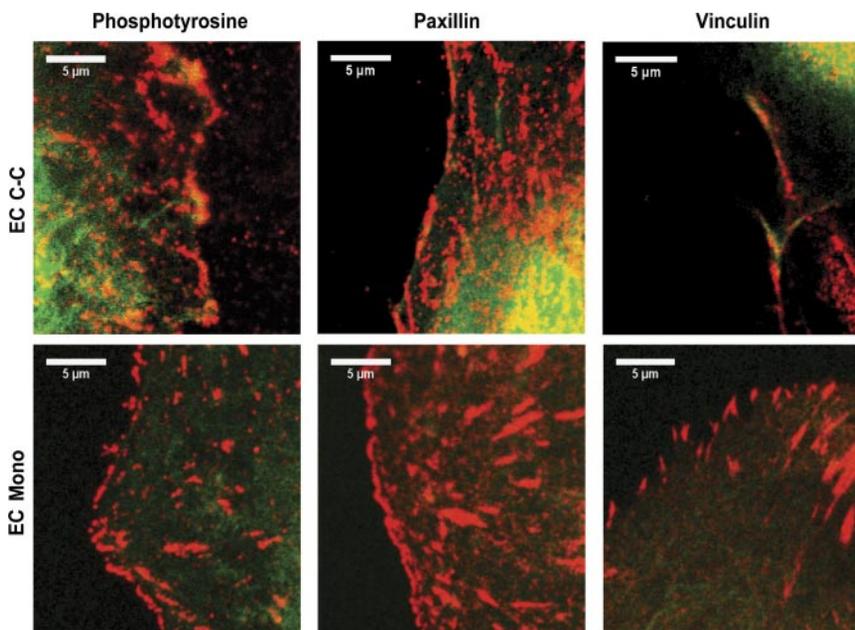

Fig. 2. Focal complex formation after 1 h of EC spreading in coculture (EC C-C) and monoculture (EC Mono) was determined by immunofluorescence. After 1 h, ECs in monoculture have begun to form focal adhesions, whereas ECs in coculture have only formed focal complexes. ECs in coculture had similar amounts of phosphotyrosine and paxillin located at the cell periphery but less vinculin compared with ECs in monoculture. Adhesion proteins stained red and cells stained green.
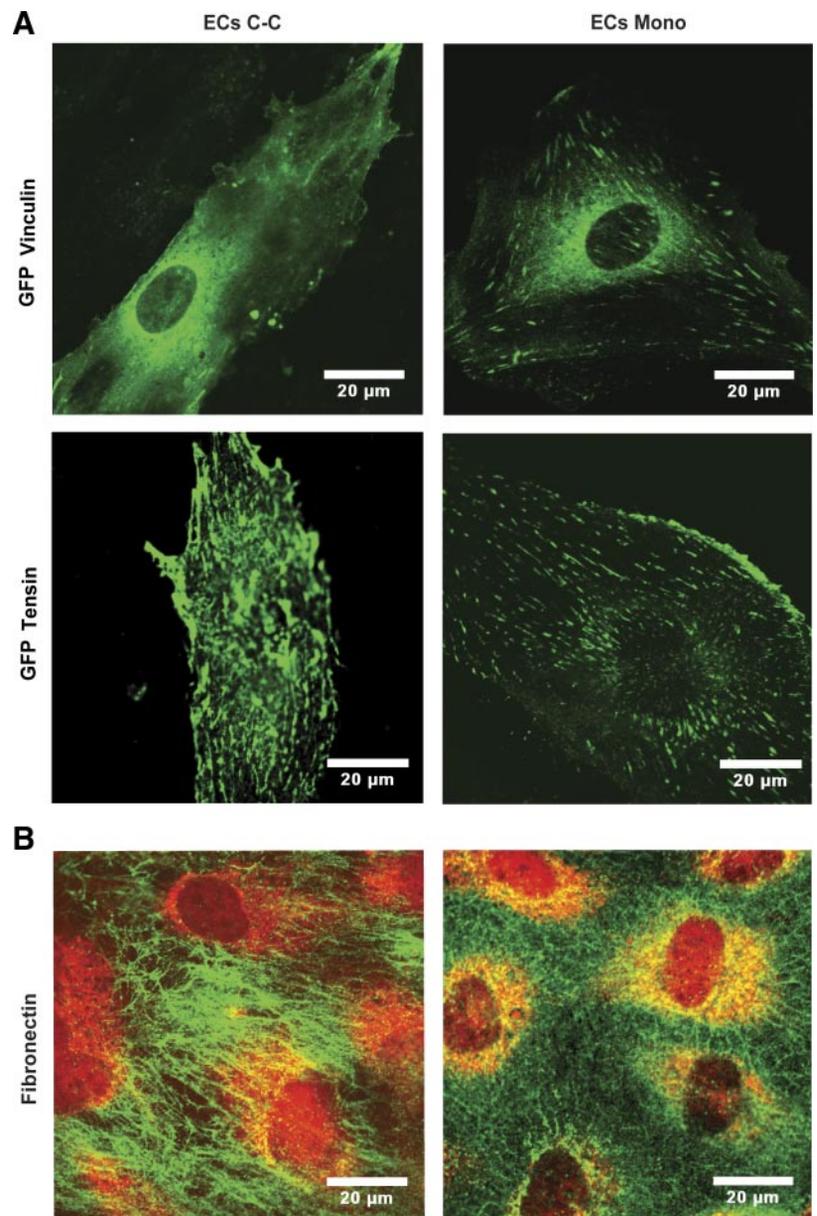
Fig. 3. Focal and fibrillar adhesion formation were determined by immunofluorescence and green fluorescent protein (GFP) labeling. ECs in coculture did not form focal adhesions 4 h after attachment, as indicated by diffuse GFP-vinculin fluorescence, whereas ECs in monoculture formed many focal adhesions. ECs in coculture formed fibrillar adhesions 4 h after attachment, as indicated by positive GFP-tensin at the centrally located elongated adhesions, whereas ECs in monoculture did not form fibrillar adhesions (*A*). After 2 days of attachment, ECs in monoculture had reorganized some FN into small fibrils, whereas an abundant amount of fibrillar FN was found between ECs and SMCs in coculture (*B*). FN stained green and ECs stained red.

a significantly higher amount of tensin. The gene expression of many molecules involved in focal adhesion and fibrillar adhesion formation was determined 3 days after coculture formation (*n* = 5; Fig. 4*B*). Consistent with focal adhesion protein expression, ECs in coculture had significantly reduced mRNA levels of molecules associated with focal adhesion formation compared with ECs in monoculture. Interestingly, FAK gene expression was similar within ECs on SMCs and FN-coated plastic. Tensin protein and gene expression within ECs were significantly increased in coculture compared with monoculture.

Substrate rigidity alone does not dictate EC spreading or focal adhesion formation in coculture. We hypothesized that ECs in coculture had reduced cell areas and lacked focal adhesions due to the stiffness of underlying SMCs. We measured the apparent elastic modulus of SMCs with an AFM at various time points after serum starvation (*n* = 3–4; Fig. 5*A*). The apparent elastic modulus did not significantly change from

2 to 9 days of serum starvation. Thus, the data were pooled, and the apparent elastic modulus of SMCs was found to be 1.98 ± 0.26 kPa (*n* = 10). Polyacrylamide gels were made with 5% acrylamide and various bis-acrylamide concentrations yielding substrates of similar elastic moduli to SMCs (*n* = 3–7; Fig. 5*B*). The relationship between elastic modulus and bis-acrylamide concentration was similar to previously published results (7). FN was cross-linked to the surface of gels to promote attachment to polyacrylamide. Since immobilized FN can inhibit fibrillar adhesion formation, some of the gels with cross-linked FN were incubated three additional times with FN to build a denser FN matrix and promote fibrillar adhesion formation.

EC spreading rates on SMCs (*n* = 5) and gels (*n* = 5) of similar elastic moduli as SMCs are shown in Fig. 6. The addition of three additional coatings of FN did not alter the spreading rate of ECs; thus, we pooled the data. As expected, the EC spreading rate increased as the stiffness of the gel
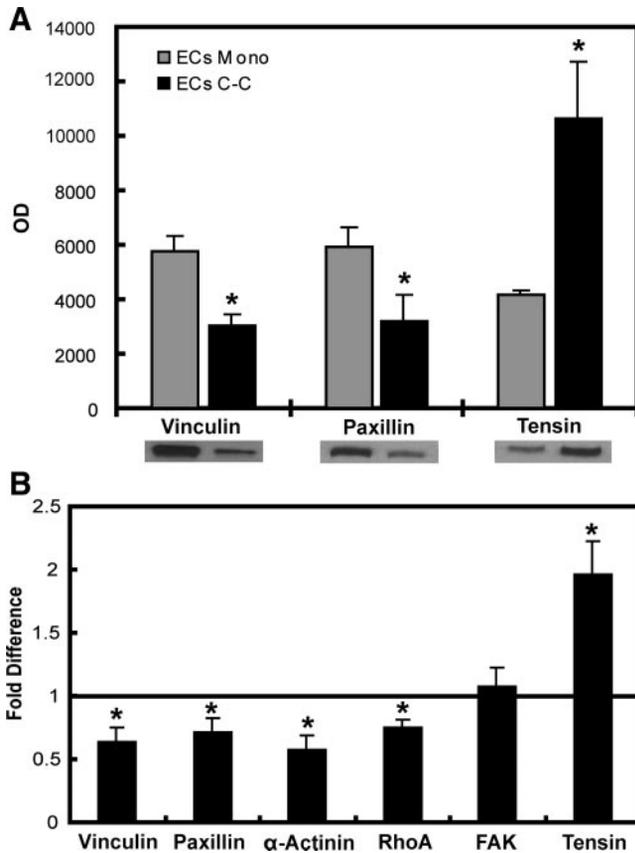
Fig. 4. Protein and gene expression profiles of common molecules found in either fibrillar or focal adhesions were determined in ECs adhered to SMCs or FN-coated plastic. After 2 days in culture, EC focal adhesion proteins in coculture were significantly reduced relative to ECs in monoculture, whereas tensin was significantly increased compared with ECs in monoculture ($n = 3$; *A*). After 3 days in culture, tensin gene expression was significantly increased, whereas the gene expression of many molecules involved with the formation of focal adhesions were significantly decreased within ECs in coculture ($n = 5$; *B*). The gene expression data shown are for ECs in coculture relative to ECs in monoculture. OD, optical density units. *$P < 0.05$ compared with ECs in monoculture.

increased, but the EC spreading rate on SMCs was significantly lower than the spreading rate on gels of similar elastic moduli, as indicated by the separate populations shown in Fig. 6. The linear regression curves formed from the gel data were used to predict the EC spreading rate when adhered to a substrate with an elastic modulus of 1.98 kPa (SMC elastic modulus). The predicted spreading rates were significantly greater than the actual EC spreading rates found in coculture. The EC spreading rate on SMCs was equivalent to gels with an elastic modulus about one-half the value obtained with SMCs. Thus, the SMC rigidity is not the only contributor to the reduced EC spreading on SMCs.

We also hypothesized that the lack of focal adhesions within ECs in coculture was due to the "softness" of the underlying SMCs. To test this hypothesis, we performed vinculin and paxillin immunostaining on subconfluent ECs that had spread for 4 h (Fig. 7) or fully confluent ECs after 2 days of attachment on polyacrylamide gels. The vinculin plaque size was measured to determine the focal adhesion area ($n = 3$; Fig. 8). Consistent with the literature (22), we found that focal adhesion size increased as the stiffness of the gel increased. Sub-

confluent spreading ECs formed larger focal adhesions than fully confluent ECs. Although small in size, focal adhesions formed within ECs adhered to the softest gels (0.41 and 0.86 kPa), whereas ECs that adhered to the more rigid SMCs (1.98 kPa) lacked focal adhesions (Fig. 3). Therefore, the softness of SMCs alone does not explain the lack of EC focal adhesions found in coculture.

DISCUSSION

In this study, we found that ECs in coculture lacked focal adhesions and had a reduced spreading rate compared with ECs adhered to polyacrylamide gels of similar stiffness as underlying SMCs in coculture. ECs in coculture attached and spread along SMCs primarily through the $\alpha_5\beta_1$-integrin complex. Interactions between $\alpha_5\beta_1$-integrin and fibrillar FN on the surface of SMCs induced the rapid formation of fibrillar adhesions and led to a reduction in focal adhesion protein expression. The lack of focal adhesions and abundance of fibrillar adhesions in coculture was not a transient observation, as indicated by immunostaining after 2 days of culture. Despite this shift in the adhesion mechanism, we (28) have previously found that ECs attached to SMCs can resist shear stresses as high as 300 dyn/cm^2.
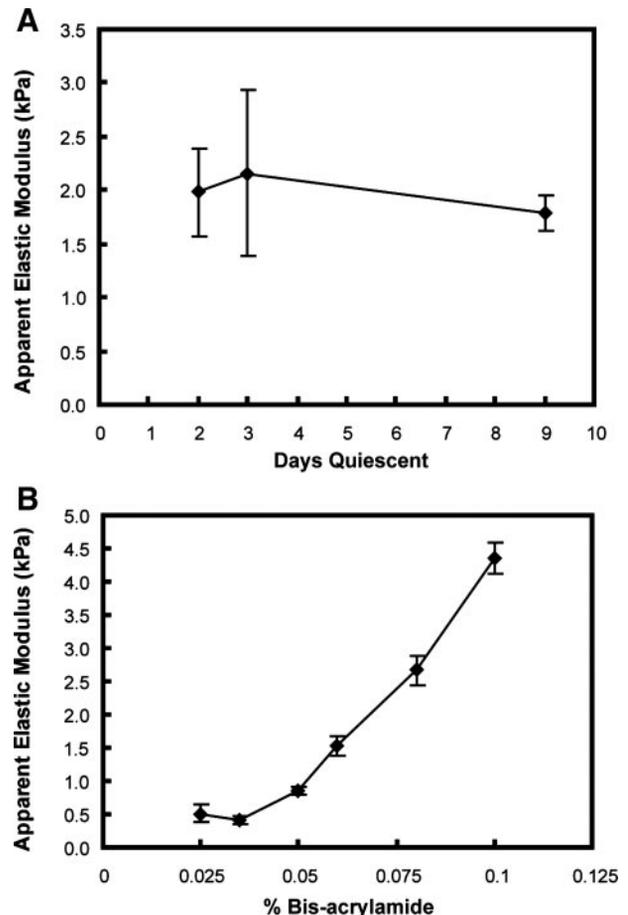

Fig. 5. Atomic force microscopy was used to determine the apparent elastic modulus of SMCs and various polyacrylamide gels. The apparent elastic modulus of quiescent SMCs did not significantly change from 2 to 9 days of serum starvation ($n = 3$–4; *A*). Polyacrylamide gels made with 5% acrylamide and varying concentrations of bis-acrylamide formed substrates with varying elastic moduli, as measured by atomic force microscopy ($n = 3$–7; *B*).
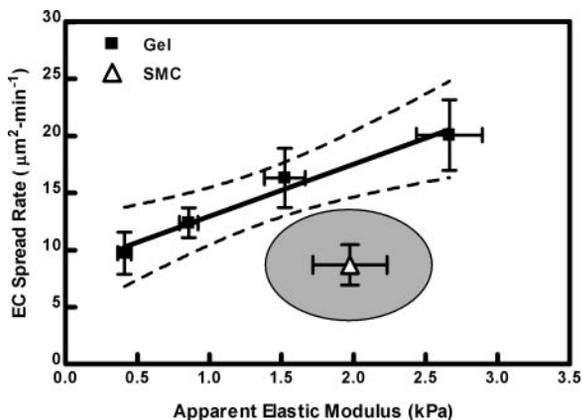
Fig. 6. EC spreading rates were measured when ECs were adhered to SMCs or polyacrylamide gels with elastic moduli similar to SMCs. Points represent averages of 5 separate experiments at each condition. EC spreading rates increased with the stiffness of the polyacrylamide gel. The EC spreading rate on SMCs was significantly lower than that predicted by gels of similar elastic moduli. The 95% confidence limits are indicated by the dashed lines and shaded oval.
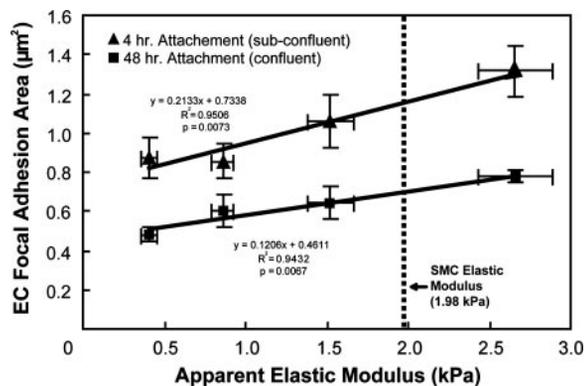

Fig. 8. The size of the EC focal adhesions depends on the elastic modulus of polyacrylamide gels. Points represent averages of 3 separate experiments at each elastic modulus. The focal adhesion area increased as the stiffness of the polyacrylamide gel increased with and without additional layers of adsorbed FN. Both slopes were found to be statistically significant.

The results from this study illustrate that the FN receptor, $\alpha_5\beta_1$-integrin, is the primary integrin complex responsible for EC attachment and spreading in coculture. While $\alpha_v\beta_3$-integrin aided EC attachment in coculture, it did not appear to affect cell spreading in coculture. The role of $\alpha_5\beta_1$- and $\alpha_v\beta_3$-integrin in EC attachment and spreading on FN-coated plastic was very similar to that of ECs in coculture, indicating that FN on the surface of SMCs is the major ECM protein that controls EC attachment and spreading in coculture. TEBVs, like native arteries, produce significant amounts of FN mRNA and protein

(11). Thus, EC interactions with FN in coculture may be relevant to TEBVs and native arteries. These results, along with previous findings (28), indicate that $\alpha_5\beta_1$-integrin binds to fibrillar FN on the surface of underlying SMCs and directs ECs to spread along the surface of SMCs orienting in the direction of fibrillar FN. Katz et al. (14) found that classical focal adhesions containing $\alpha_v\beta_3$-integrin did not coincide with fibrillar FN. The reduced role of EC $\alpha_v\beta_3$-integrin in coculture could be due to the fibrillar organization of FN as well as the threefold lower surface protein expression of $\alpha_v\beta_3$-integrin compared with $\alpha_5\beta_1$-integrin after trypsinization (data not shown).
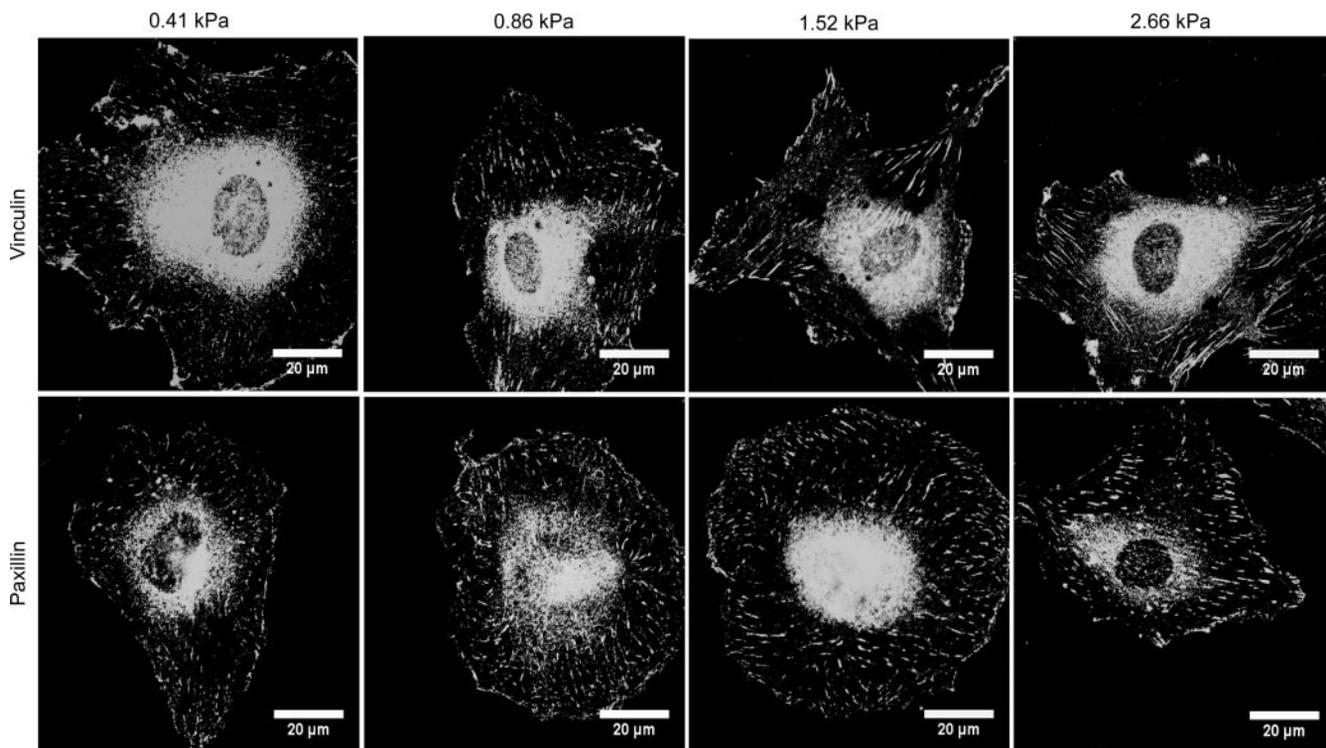

Fig. 7. Focal adhesion formation on polyacrylamide gels with similar elastic moduli as SMCs was determined by immunofluorescence. ECs formed more elongated focal adhesions as the stiffness of the polyacrylamide gels increased, as indicated by vinculin and paxillin immunofluorescence after 4 h of attachment. ECs formed focal adhesions on polyacrylamide gels of similar elastic moduli as SMCs.

The extracellular integrin domains bind to the ECM on the substrate, whereas the cytoplasmic domains interact with various adhesion proteins. As the cell spreads, the cytoplasmic integrin domains interact with adhesion proteins to form focal complexes at the leading edge. Focal complexes mature and form focal adhesions during cell spreading. The maturation process involves a temporal recruitment of different adhesion proteins. The proteins recruited to these sites first include $\alpha_v\beta_3$-integrin and phosphotyrosine, with paxillin following shortly thereafter (31). Later in the maturation process, vinculin is recruited (31), and if the cell generates enough tension along the actin filaments, then focal adhesions form. We found that ECs adhered to FN-coated plastic or SMCs recruited similar amounts of phosphotyrosine and paxillin to the leading edge, but there seemed to be less vinculin recruited to the leading edge of ECs in coculture than in monoculture. In addition, ECs that adhered to FN-coated plastic rapidly formed focal adhesions, whereas ECs in coculture did not form focal adhesions. Thus, the lower levels of vinculin recruitment in coculture could lead to an inhibition of the maturation process to form focal adhesions. The limited maturation of focal complexes in coculture could be due to the lack of $\alpha_v\beta_3$-integrin interactions with the ECM and the lower substrate stiffness in coculture.

We found that ECs in coculture have lower cell spreading rates compared with ECs on polyacrylamide gels with a similar stiffness as SMCs. Although ECs plated on SMCs (1.98 kPa) did not form any focal adhesions, focal adhesions formed in ECs plated on polyacrylamide gels with an elastic modulus between 0.41 to 2.66 kPa. After 2 days in culture, ECs in coculture had reduced levels of paxillin and vinculin gene and protein expression compared with ECs in monoculture. Although vinculin-deficient cells spread to half the size of wild-type cells (8), ECs that attached to FN-coated plastic or SMCs in the present study likely had similar levels of vinculin during the initial stage of spreading.

Results from several studies, all of which were performed on synthetic substrates, have suggested that substrate rigidity plays a major role in cell spreading and focal adhesion formation (7, 13, 22, 30). Our spreading and focal adhesion results on polyacrylamide gels agree with the literature, but our results of EC spreading and adhesion formation on SMCs indicate that substrate rigidity plays a limited role in spreading and focal adhesion formation in coculture. Thus, there are additional interactions between the cells in coculture that reduce cell spreading and inhibit focal adhesion formation. The fibrillar organization of FN on the surface of SMCs could limit the interactions of $\alpha_v\beta_3$-integrin with the ECM, thus reducing focal adhesion formation. In addition, the uneven topography of the underlying fibrillar FN and SMCs could further decrease cell spreading and limit focal adhesion formation. It has been shown that the uneven topography (islands with 2-μm diameter and 95-nm height) created on synthetic surfaces reduced cell spreading and focal adhesions compared with a flat surface (4, 5). The topography on the surface of SMCs could have local variations of several micrometers, thus decreasing EC spreading and focal adhesion formation. Altering glucose concentrations may modulate the effect of FN topography and alter EC spreading rates (10, 15). A functional TEBV must have mechanical properties similar to native vessels, and to increase strength of the vessel wall through collagen production, re-

searchers have exposed the vessels to cyclic strains (for a review, see Ref. 19). Thus, stretch preconditioning of SMCs could also alter the organization of the ECM, thus altering EC spreading rates and adhesion mechanisms in coculture.

Focal adhesions may be affected by metabolic products from SMCs. For example, 12-hydroxyeicosatetraenoic acid [12(S)-HETE], a lipoxygenase metabolite of arachidonic acid, decreased $\alpha_v\beta_3$-integrin- and vinculin-containing focal adhesions within ECs up to 4 h after 12(S)-HETE treatment (26, 27), but 24 h after the removal of 12(S)-HETE, ECs recovered their $\alpha_v\beta_3$-integrin-containing focal adhesions (26). SMCs maintained in medium containing lower glucose concentrations (5 mM) produced significantly less 12(S)-HETE than those maintained in media with higher glucose concentrations (23 mM) (1). Therefore, the high glucose concentration (17.5 mM) in the quiescent media could stimulate SMCs to produce a significant amount of 12(S)-HETE (1), which could decrease initial EC focal adhesion formation in coculture. The effect of glucose concentration on 12(S)-HETE production and reduced focal adhesion formation does not explain the lack of focal adhesions after 2 days in coculture since the glucose concentration in coculture media is 5.6 mM. The effect of 12(S)-HETE on fibrillar adhesion formation is not known.

Focal adhesion formation depends on the cell's ability to generate the necessary contractile forces within the cell. Contractile forces are generated by interactions between actin and myosin due to myosin ATPase activity. Myosin ATPase activity is regulated by myosin light chain phosphorylation, which has been found to be enhanced by Rho (for a review, see Ref. 29). Clustering of β_3-integrins can activate RhoA (2), whereas clustering of β_1-integrins suppresses RhoA activation (20). Our results suggest that the elastic modulus of cellular substrates is only one of many factors, such as eicosaniod mediators, surface topography, and ECM organization, that modulate cell behavior. Therefore, we hypothesize that SMC rigidity, topography, eicosaniod production, and surface ECM organization limit EC spreading by inhibiting β_3-integrin clustering and promoting β_1-integrin clustering, which, in turn, suppresses RhoA production and activity to a point where the actin cytoskeleton cannot generate enough tension to form focal adhesions and continue spreading. In turn, there is a reduced recruitment of paxillin and vinculin to these adhesions, leading to their downregulation.

The lack of focal adhesions and abundance of fibrillar adhesions found within ECs adhered to SMCs may have important functional implications. Tensin, the major protein in fibrillar adhesions, may be involved with signal transduction since it contains a Src homology 2 (SH2) domain and can be phosphorylated on tyrosine, serine, and threonine residues (for a review, see Ref. 18). FAK also contains a SH2 domain, which can act as a docking site of many different signaling molecules. For example, blockade of FAK-dependent signaling in coronary arterioles reduced endothelial nitric oxide synthase (eNOS) activity, and it was proposed that FAK interacts with the well-established shear stress-induced kinase cascade of Src, phosphoinositide 3-kinase, Akt, and eNOS (16). Therefore, the composition of the proteins at EC adhesion sites has the potential to regulate many important signaling mechanisms controlling EC function.

REFERENCES

1. **Alpert E, Gruzman A, Totary H, Kaiser N, Reich R, Sasson S.** A natural protective mechanism against hyperglycaemia in vascular endothelial and smooth-muscle cells: role of glucose and 12-hydroxyeicosatetraenoic acid. *Biochem J* 362: 413–422, 2002.

2. **Avalos AM, Arthur WT, Schneider P, Quest AF, Burridge K, Leyton L.** Aggregation of integrins and RhoA activation are required for Thy-1-induced morphological changes in astrocytes. *J Biol Chem* 279: 39139–39145, 2004.

3. **Brown M, Wallace CS, Truskey GA.** Vascular endothelium. In: *Wiley Encyclopedia of Biomedical Engineering*, edited by Akay M. Indianapolis, IN: Wiley, 2006.

4. **Dalby MJ, Childs S, Riehle MO, Johnstone HJ, Affrossman S, Curtis AS.** Fibroblast reaction to island topography: changes in cytoskeleton and morphology with time. *Biomaterials* 24: 927–935, 2003.

5. **Dalby MJ, Riehle MO, Johnstone HJ, Affrossman S, Curtis AS.** Polymer-demixed nanotopography: control of fibroblast spreading and proliferation. *Tissue Eng* 8: 1099–1108, 2002.

6. **Discher DE, Janmey P, Wang YL.** Tissue cells feel and respond to the stiffness of their substrate. *Science* 310: 1139–1143, 2005.

7. **Engler A, Bacakova L, Newman C, Hategan A, Griffin M, Discher D.** Substrate compliance versus ligand density in cell on gel responses. *Biophys J* 86: 617–628, 2004.

8. **Ezzell RM, Goldmann WH, Wang N, Parasharama N, Ingber DE.** Vinculin promotes cell spreading by mechanically coupling integrins to the cytoskeleton. *Exp Cell Res* 231: 14–26, 1997.

9. **Form DM, Pratt BM, Madri JA.** Endothelial cell proliferation during angiogenesis. In vitro modulation by basement membrane components. *Lab Invest* 55: 521–530, 1986.

10. **Giannico G, Cortes P, Baccora MH, Hassett C, Taube DW, Yee J.** Glibenclamide prevents increased extracellular matrix formation induced by high glucose concentration in mesangial cells. *Am J Physiol Renal Physiol* 292: F57–F65, 2007.

11. **Heydarkhan-Hagvall S, Esguerra M, Helenius G, Soderberg R, Johansson BR, Risberg B.** Production of extracellular matrix components in tissue-engineered blood vessels. *Tissue Eng* 12: 831–842, 2006.

12. **Isenberg BC, Williams C, Tranquillo RT.** Small-diameter artificial arteries engineered in vitro. *Circ Res* 98: 25–35, 2006.

13. **Jiang G, Huang AH, Cai Y, Tanase M, Sheetz MP.** Rigidity sensing at the leading edge through alphavbeta3 integrins and RPTPalpha. *Biophys J* 90: 1804–1809, 2006.

14. **Katz BZ, Zamir E, Bershadsky A, Kam Z, Yamada KM, Geiger B.** Physical state of the extracellular matrix regulates the structure and molecular composition of cell-matrix adhesions. *Mol Biol Cell* 11: 1047–1060, 2000.

15. **Ko SH, Hong OK, Kim JW, Ahn YB, Song KH, Cha BY, Son HY, Kim MJ, Jeong IK, Yoon KH.** High glucose increases extracellular matrix production in pancreatic stellate cells by activating the renin-angiotensin system. *J Cell Biochem* 98: 343–355, 2006.

16. **Koshida R, Rocic P, Saito S, Kiyooka T, Zhang C, Chilian WM.** Role of focal adhesion kinase in flow-induced dilation of coronary arterioles. *Arterioscler Thromb Vasc Biol* 25: 2548–2553, 2005.

17. **Livak KJ, Schmittgen TD.** Analysis of relative gene expression data using real-time quantitative PCR and the $2(-\Delta\Delta C_T)$ method. *Methods* 25: 402–408, 2001.

18. **Lo SH.** Tensin. *Int J Biochem Cell Biol* 36: 31–34, 2004.

19. **Mitchell SL, Niklason LE.** Requirements for growing tissue-engineered vascular grafts. *Cardiovasc Pathol* 12: 59–64, 2003.

20. **O'Connor KL, Nguyen BK, Mercurio AM.** RhoA function in lamellae formation and migration is regulated by the alpha6beta4 integrin and cAMP metabolism. *J Cell Biol* 148: 253–258, 2000.

21. **Orr AW, Sanders JM, Bevard M, Coleman E, Sarembock IJ, Schwartz MA.** The subendothelial extracellular matrix modulates NF-kappaB activation by flow: a potential role in atherosclerosis. *J Cell Biol* 169: 191–202, 2005.

22. **Pelham RJ Jr, Wang Y.** Cell locomotion and focal adhesions are regulated by substrate flexibility. *Proc Natl Acad Sci USA* 94: 13661–13665, 1997.

23. **Rozen S, Skaletsky HJ.** Primer3 on the WWW for general users and for biologist programmers. In: *Bioinformatics Methods and Protocols: Methods in Molecular Biology*, edited by Krawetz S, Misener S. Totowa, NJ: Humana, 2000.

24. **Sastry SK, Burridge K.** Focal adhesions: a nexus for intracellular signaling and cytoskeletal dynamics. *Exp Cell Res* 261: 25–36, 2000.

25. **Sato M, Theret DP, Wheeler LT, Ohshima N, Nerem RM.** Application of the micropipette technique to the measurement of cultured porcine aortic endothelial cell viscoelastic properties. *J Biomech Eng* 112: 263–268, 1990.

26. **Tang DG, Chen YQ, Diglio CA, Honn KV.** Protein kinase C-dependent effects of 12(S)-HETE on endothelial cell vitronectin receptor and fibronectin receptor. *J Cell Biol* 121: 689–704, 1993.

27. **Tang DG, Diglio CA, Honn KV.** 12(S)-HETE-induced microvascular endothelial cell retraction results from PKC-dependent rearrangement of cytoskeletal elements and alpha V beta 3 integrins. *Prostaglandins* 45: 249–267, 1993.

28. **Wallace CS, Champion JC, Truskey GA.** Adhesion and function of human endothelial cells co-cultured on smooth muscle cells. *Ann Biomed Eng* 35: 375–386, 2007.

29. **Wozniak MA, Modzelewska K, Kwong L, Keely PJ.** Focal adhesion regulation of cell behavior. *Biochim Biophys Acta* 1692: 103–119, 2004.

30. **Yeung T, Georges PC, Flanagan LA, Marg B, Ortiz M, Funaki M, Zahir N, Ming W, Weaver V, Janmey PA.** Effects of substrate stiffness on cell morphology, cytoskeletal structure, and adhesion. *Cell Motil Cytoskeleton* 60: 24–34, 2005.

31. **Zaidel-Bar R, Ballestrem C, Kam Z, Geiger B.** Early molecular events in the assembly of matrix adhesions at the leading edge of migrating cells. *J Cell Sci* 116: 4605–4613, 2003.

32. **Zaidel-Bar R, Cohen M, Addadi L, Geiger B.** Hierarchical assembly of cell-matrix adhesion complexes. *Biochem Soc Trans* 32: 416–420, 2004.

33. **Zamir E, Katz M, Posen Y, Erez N, Yamada KM, Katz BZ, Lin S, Lin DC, Bershadsky A, Kam Z, Geiger B.** Dynamics and segregation of cell-matrix adhesions in cultured fibroblasts. *Nat Cell Biol* 2: 191–196, 2000.